arXiv:1512.08729v1 [physics.atom-ph] 1 Nov 2015

TaN, a molecular system for probing $\mathcal{P},\mathcal{T}$-violating hadron physics

Timo Fleig,[1,*] Malaya K. Nayak,[2,1,†] and Mikhail Kozlov[3,4,‡]

[1] *Laboratoire de Chimie et Physique Quantiques, IRSAMC, Université Paul Sabatier Toulouse III, 118 Route de Narbonne, F-31062 Toulouse, France*
[2] *Bhabha Atomic Research Centre, Trombay, Mumbai - 400085, India*
[3] *Petersburg Nuclear Physics Institute, Gatchina 188300, Russia*
[4] *St. Petersburg Electrotechnical University "LETI", Professor Popov Street 5, St. Petersburg 197376, Russia*

(Dated: December 31, 2015)

All-electron configuration interaction theory in the framework of the Dirac-Coulomb Hamiltonian has been applied to the TaN molecule, a promising candidate in the search for Beyond-Standard-Model physics in both the hadron and the lepton sector of matter. We obtain in the first excited $^3\Delta_1$ state a $\mathcal{P},\mathcal{T}$-odd effective electric field of 36.0 $\left[\frac{\mathrm{GV}}{\mathrm{cm}}\right]$, a scalar-pseudoscalar $\mathcal{P},\mathcal{T}$-odd interaction constant of 32.8 [kHz], and a nuclear magnetic-quadrupole moment interaction constant of 0.74 $\left[\frac{10^{33}\mathrm{Hz}}{e\,\mathrm{cm}^2}\right]$. The latter interaction constant has been obtained with a new approach which we describe in detail. Using the same highly correlated all-electron wavefunctions with up to 2.5 billion expansion terms, we obtain a parallel magnetic hyperfine interaction constant of -2954 [MHz] for the ^{181}Ta nucleus, a very large molecule-frame electric dipole moment of -4.91 [Debye], and spectroscopic constants for the four lowest-lying electronic states of the molecule.

INTRODUCTION

Electric Dipole Moments (EDMs) are sensitive low-energy probes for New Physics, i.e., physics beyond the Standard Model (SM) of elementary particles [1]. The existence of an EDM gives rise to $\mathcal{P}$- (spatial parity) and $\mathcal{T}$- (time-reversal) odd interactions [2] which originate in fundamental sources of $(\mathcal{CP})$-violation [3] and are related to these via the $\mathcal{CPT}$-theorem [4].

Atomic and molecular systems allow for probing $(\mathcal{CP})$-violation both in the lepton as well as the hadron sector of matter. In the former case, typically the electron EDM and the electron-nucleon scalar-pseudoscalar (eN-SPS) interaction are investigated [5]. These two effects are in general the dominant expected manifestations of $\mathcal{P},\mathcal{T}$-violation in paramagnetic systems [6–8]. Concerning the latter, possible important sources of symmetry-violating effects at the atomic scale are the nuclear Schiff moment [2, 9] and the nuclear magnetic quadrupole moment (MQM) [10], for the same underlying sources of $(\mathcal{CP})$-violation. The EDM due to a nuclear-MQM - electronic-magnetic-field interaction can for certain types of atomic and molecular systems even be larger than that due to the Schiff moment.

In the present paper we investigate the neutral diatomic molecule TaN which has been identified as a promising candidate in EDM searches [11] for various reasons. Deformed nuclei such as the ^{181}Ta nucleus exhibit a strong enhancement of the MQM relative to that of spherical nuclei, roughly one order of magnitude, which increases the prospect of measuring an ensuing $\mathcal{P},\mathcal{T}$-odd shift. The MQM is directly related to the quantum chromodynamics (QCD) $(\mathcal{CP})$-violating parameter $\tilde{\Theta}$ [12]. Furthermore, an MQM can arise *via* EDMs of the u and d quarks, $d_{u,d}$, and *via* chromo-EDMs, $\tilde{d}_{u,d}$ [13] in the framework of spontaneous $\mathcal{CP}$-violation in the Higgs sector [2]. The search for the ensuing $\mathcal{P},\mathcal{T}$-violating effects in a molecular system may, therefore, further constrain (or unravel) beyond-standard-model (BSM) hadron physics. A further asset is the electronic structure of the TaN molecule. From earlier experimental and theoretical studies it is known that TaN has an energetically very low-lying $^3\Delta$ state [14] arising mainly from a $\sigma^1\,\delta^1$ electronic configuration. In other valence-isoelectronic candidate molecules such as ThO [15–17] and HfF^+ [18, 19] this state is deeply bound and exhibits a very small magnetic moment which facilitates experimental studies and helps reduce the vulnerability of experiments to decoherence and systematic errors [20, 21].

In the present work we have pursued several goals. We have implemented the nuclear-MQM - electronic-magnetic-field interaction constant W_M as an expectation value into our four-component relativistic correlated all-electron approaches. Section documents the underlying theory, details of the implementation, as well as a brief account of the electronic-structure method for obtaining the required molecular wavefunctions. In section we present the first detailed theoretical spectroscopic study of the TaN molecule including leading relativistic effects described in the framework of four-component Dirac theory. Apart from spectroscopic constants for low-lying electronic states we also discuss computed molecular electric dipole moments and transition dipole moments. Furthermore, we present and discuss different $\mathcal{P},\mathcal{T}$-odd interaction constants relevant to the search for molecular EDMs, as well as the parallel magnetic hyperfine interaction constant for the ^{181}Ta nucleus with spin $I = 7/2$. The final section is dedicated to conclusions drawn from our present findings.

THEORY AND METHODS

Correlated Relativistic Wavefunction Method

The four-component molecular Dirac wavefunctions including the contributions of dynamic electron correlation have been obtained using a Configuration Interaction approach implemented in the `KR-CI` module [22–24] of the `Dirac11` [25] program package. Throughout the present study we have used the all-electron Dirac-Coulomb Hamiltonian operator in Born-Oppenheimer approximation

$$\hat{H}^{DC} = \sum_A \sum_i \left[c(\vec{\alpha}\cdot\vec{p})_i + \beta_i m_0 c^2 + V_{iA}\mathbb{1}_4 \right] + \sum_{i,j>i} \frac{1}{r_{ij}}\mathbb{1}_4 + \sum_{A,B>A} V_{AB}, \tag{1}$$

where V_{iA} is the potential-energy operator for electron i in the electric field of nucleus A, $\mathbb{1}_4$ is a unit 4×4 matrix and V_{AB} represents the potential energy due to the internuclear classical electrostatic repulsion of the clamped nuclei.

The molecular wavefunctions are defined as a linear expansion into Slater determinants, the latter being formed from the basis of molecular time-reversal paired 4-spinors (Kramers partners, $\{\varphi_i, \varphi_{\bar{i}}\}$), inter-related as $\hat{K}\varphi_i = \varphi_{\bar{i}}$ and $\hat{K}\varphi_{\bar{i}} = -\varphi_i$, where

$$\hat{K}(n) := e^{-\frac{\imath}{2}\pi\left(\sum\limits_{j=1}^{n} \boldsymbol{\sigma}\otimes\mathbb{1}_2(j)\right)\cdot\vec{e}_y} \prod_{j=1}^{n} \hat{K}_0(j), \tag{2}$$

where the Pauli matrices are defined for particle j in a cartesian basis and $\hat{K}_0$ is the complex conjugation operator. For the one-fermion case, setting $n = 1$ and Taylor expanding the exponential in Eq. (2) results in the one-body time-reversal operator

$$\hat{K} := -\imath\boldsymbol{\Sigma}_y\hat{K}_0 \tag{3}$$

with $\boldsymbol{\Sigma}_y = \mathbf{1}_2 \otimes \boldsymbol{\sigma}_y$ a Dirac operator.

The expansion coefficients of the molecular Kramers pairs in terms of the atomic basis sets are obtained from an all-electron Dirac-Coulomb Hartree-Fock (DCHF) calculation.

The Slater determinant expansion for the wavefunction then reads

$$|\psi_k\rangle = \sum_{I=1}^{\dim\mathcal{F}^{\mathrm{t}}(\mathrm{M,N})} c_{kI} \left|(\mathcal{S}\overline{\mathcal{T}})_I\right\rangle \tag{4}$$

with $\dim\mathcal{F}^{\mathrm{t}}(\mathrm{M,N})$ the dimension of the truncated N-particle Fock-space sector over M molecular 4-spinors and expansion coefficients c_{kI} varied by diagonalizing the matrix representation of $\hat{H}^{DC}$ in the Slater determinant basis. In this step which takes into account the correlation part of the electron-electron interaction, the determinants are represented by strings of creation operators in second quantization as

$$\left|(\mathcal{S}\overline{\mathcal{T}})\right\rangle = \mathcal{S}^\dagger\overline{\mathcal{T}}^\dagger \mid \ \rangle \tag{5}$$

where $\mathcal{S}^\dagger \mid \ \rangle = \hat{a}^\dagger_{\mathcal{S}_1}\hat{a}^\dagger_{\mathcal{S}_2}\ldots\hat{a}^\dagger_{\mathcal{S}_j} \mid \ \rangle$ and $\overline{\mathcal{T}}^\dagger \mid \ \rangle = \hat{a}^\dagger_{\overline{\mathcal{T}}_1}\hat{a}^\dagger_{\overline{\mathcal{T}}_2}\ldots\hat{a}^\dagger_{\overline{\mathcal{T}}_{N-j}} \mid \ \rangle$ and N is the number of explicitly treated electrons. Axial molecular double-group (in the present case the subgroup C^*_{64v} [26]) and time-reversal symmetry have been exploited.

Nuclear magnetic quadrupole moment interaction

Basic theory

The effective Hamiltonian for the interaction of a nuclear magnetic quadrupole moment with an electronic magnetic field is [11]

$$\hat{H}_{\mathrm{MQM}} = -\frac{W_M\, M}{2I\,(2I-1)}\,\vec{J}_e\hat{T}\vec{n} \tag{6}$$

where $\vec{J}_e$ denotes electronic angular momentum and $\mathbf{M}$ is the second-rank nuclear magnetic quadrupole moment tensor [10] with components

$$M_{mk} = \frac{3M}{2I(2I-1)}\,T_{mk} = \frac{3}{2}\,\frac{M}{I(2I-1)}\,\left[I_mI_k + I_kI_m - \frac{2}{3}\,I(I+1)\delta_{mk}\right] \tag{7}$$

with $\mathbf{I}$ the nuclear angular momentum and M the magnitude of the nuclear MQM. For instance, if $I_k = I$ along the internuclear vector $\vec{n}$ and $I_{i\neq k} = 0$ then $T_{kk} = \frac{I}{3}\,(4I-2)$ and $M_{kk} = M$. The ensuing MQM energy shift results to $\Delta E_{MQM} = -\frac{1}{3}\,W_M M\Omega$ with $\Omega := \vec{J}_e\cdot\vec{n}$.

The nuclear MQM has two contributions [27]. The first contribution is due to a possible nucleon EDM, proportional to $d_n < 10^{-25}\,e$ cm. The second is due to a $\mathcal{P},\mathcal{T}$-odd nuclear potential, proportional to the Fermi constant, order of magnitude $G_F \approx 10^{-37}$ eV cm^3. Due to the smallness

of the ensuing energy shift and the typical energy differences $E_\Omega - E_{\Omega'}$ between electronic states in diatomic molecules — expressed in a basis of Hund's case C functions —, on the order of eV, higher-order corrections of the type

$$E^{(2)}_{\mathrm{MQM}}(\Omega_j) = \sum_{k\neq j} \frac{\left|\left\langle \Omega_j|\hat{H}_{\mathrm{MQM}}|\Omega_k\right\rangle\right|^2}{E^{(0)}_{\Omega_j} - E^{(0)}_{\Omega_k}} \tag{8}$$

to $E^{(0)}_{\Omega_j}$ are extremely small and may safely be neglected. Considering the case of a doublet $\{|\Omega_j\rangle, |-\Omega_j\rangle\}$, $(\Omega > 0)$, the corresponding electronic energies $E(\Omega_j)_+$ and $E(\Omega_j)_-$ are near-degenerate for a free molecule, the splitting due to Ω-doubling being typically on the order of tenths of inverse centimeters for Δ states [28], or less. In the presence of an external electric field and assuming perfect polarization [6] of the molecule, $\{|\Omega_j\rangle, |-\Omega_j\rangle\}$ eigenstates are restored, exhibiting a convenient (but small) Stark splitting. In this two-dimensional subspace, $\left\langle \Omega_j \left|\hat{H}_{\mathrm{MQM}}\right| -\Omega_j\right\rangle = \left\langle -\Omega_j \left|\hat{H}_{\mathrm{MQM}}\right| \Omega_j\right\rangle = 0$ due to rotational invariance of $\hat{H}_{\mathrm{MQM}}$ for $\vec{J}_e$ the generator of rotation. Furthermore, due to

$$\left\langle -\Omega_j \left|\hat{H}_{\mathrm{MQM}}\right| -\Omega_j\right\rangle = \left\langle \Omega_j \left|\hat{P}^\dagger \hat{H}_{\mathrm{MQM}} \hat{P}\right| \Omega_j\right\rangle = -\left\langle \Omega_j \left|\hat{H}_{\mathrm{MQM}}\right| \Omega_j\right\rangle$$

and

$$\left\langle -\Omega_j \left|\hat{H}_{\mathrm{MQM}}\right| -\Omega_j\right\rangle = \left\langle \Omega_j \left|\hat{K}^\dagger \hat{H}_{\mathrm{MQM}} \hat{K}\right| \Omega_j\right\rangle^* = -\left\langle \Omega_j \left|\hat{H}_{\mathrm{MQM}}\right| \Omega_j\right\rangle^*$$

with $\hat{P}$ the operator of spatial inversion, only one matrix element, $\left\langle \Omega_j \left|\hat{H}_{\mathrm{MQM}}\right| \Omega_j\right\rangle$, needs to be calculated for the subspace [29].

The nuclear-MQM electronic-magnetic-field interaction constant

Be M_{nk} a component of the magnetic quadrupole moment due to a nuclear charged current. Then the i-th component of the quadrupole term of the associated classical vector potential is written as [10]

$$A_Q(\vec{r})_\imath \;=\; -\frac{1}{6}\sum_{k,l,n} \varepsilon_{\imath ln}\, M_{nk}\, \frac{\partial}{\partial r_l}\frac{\partial}{\partial r_k}\frac{1}{r} = \frac{1}{6}\sum_{k,l,n} \varepsilon_{\imath ln}\, M_{nk} \left(\frac{\delta_{kl}}{r^3} - \frac{3r_k r_l}{r^5}\right) \tag{9}$$

for positions $\vec{r}$ outside of the nuclear current distribution. Since M is a symmetric tensor, the nuclear vector potential thus becomes

$$\vec{A}_Q(\vec{r}) = -\sum_{k,n} M_{nk}\, \frac{1}{2r^5} \sum_{\imath,l} \varepsilon_{\imath ln}\, r_l r_k \vec{e}_\imath \tag{10}$$

The potential energy due to an electron moving with velocity $\vec{v}$ relative to the origin of this vector potential, $V_{Qe} = -\frac{e}{c}\,\vec{v}\cdot\vec{A}_Q(\vec{r})$ can now be quantized for a Dirac particle via $\vec{v} \to c\vec{\alpha}$, yielding the corresponding Hamiltonian operator, in atomic units

$$\hat{H}_{Qe} = \sum_{k,n} M_{nk}\, \frac{1}{2r^5} \sum_{\imath,j,l} \varepsilon_{\imath ln}\, r_l r_k\, \vec{e}_\imath \cdot \vec{e}_j\, \alpha_j = \sum_{j,k,l,n} \frac{1}{2r^5}\, \varepsilon_{jln}\, \alpha_j\, r_l r_k\, M_{kn} \tag{11}$$

Now, introducing a contracted tensor $(r\vec{M}) = \sum_\imath \vec{e}_\imath\, (rM)_\imath$, Eq. (11) can be rewritten as

$$\hat{H}_{Qe} = \sum_{j,l,n} \frac{1}{2r^5}\, \varepsilon_{jln}\, \alpha_j\, r_l\, \vec{e}_n \cdot \left(r\vec{M}\right) = \frac{\vec{\alpha}\times\vec{r}}{2r^5} \cdot \left(r\vec{M}\right). \tag{12}$$

This Hamiltonian can be introduced as a perturbation operator for a single Dirac particle interacting with a nuclear MQM. With regard to Eqs. (6) and (7), and Eq. (12) the nuclear-MQM

electronic-magnetic-field interaction constant is defined for a many-electron molecular system with axial symmetry as

$$W_M := \frac{3}{2\Omega} \left\langle \Psi_\Omega \left| \sum_{j=1}^{n} \left(\frac{\boldsymbol{\alpha}_j \times \mathbf{r}_{jA}}{r_{jA}^5} \right)_k (r_{jA})_k \right| \Psi_\Omega \right\rangle \tag{13}$$

for nucleus A, where j is an electron index, k a cartesian component, $\boldsymbol{\alpha}$ is a Dirac matrix, and $\Omega = \langle \mathbf{J}_\mathrm{e} \cdot \mathbf{n} \rangle$ is the projection of the total electronic angular momentum $\mathbf{J}_\mathrm{e}$ onto the molecular axis $\mathbf{n}$. In the present case, the nuclei of Ta and N are placed along the z axis, and so $\mathbf{n} = \mathbf{e}_z$.

With the wavefunctions defined in subsection the evaluation of the MQM interaction constant can be written as

$$W_M(\Psi_k) = \frac{3}{2\Omega} \sum_{I,J=1}^{\dim \mathcal{F}^\mathrm{t}(\mathrm{M,N})} c_{kI}^* c_{kJ} \left\langle (\mathcal{S}\overline{\mathcal{T}})_I \right| \sum_{j=1}^{n} \left(\frac{\boldsymbol{\alpha}_j \times \mathbf{r}_{jA}}{r_{jA}^5} \right)_l (r_{jA})_l \left| (\mathcal{S}\overline{\mathcal{T}})_J \right\rangle \tag{14}$$

with optimized CI coefficients $\{c_{kM}\}$ for the kth N-electron state ψ_k in irreducible representation Ω.

The perturbative operator in Eq. (14) is a manifestly $\mathcal{P},\mathcal{T}$-odd one-electron operator that in a basis of time-reversal paired molecular spinors can be written in second quantization as

$$\hat{H}^M = \sum_{p,q=1}^{P_u} h_{pq}^M \, a_p^\dagger a_q + \sum_{p=1}^{P_u} \sum_{q=P_u+1}^{P} h_{p\overline{q}}^M \, a_p^\dagger a_{\overline{q}} + \sum_{p=P_u+1}^{P} \sum_{q=1}^{P_u} h_{\overline{p}q}^M \, a_{\overline{p}}^\dagger a_q + \sum_{p,q=P_u+1}^{P} h_{\overline{p}\overline{q}}^M \, a_{\overline{p}}^\dagger a_{\overline{q}} \tag{15}$$

where $P_{u(b)}$ is the number of Kramers unbarred (barred) spinors in the molecular basis set and $P = P_u + P_b$. We write Eq. (14) using the first term in Eq. (15) to illustrate the computation of the expectation value:

$$W_M(\Psi_k)_1 = \frac{3}{2\Omega} \sum_{I,J=1}^{\dim \mathcal{F}^\mathrm{t}(\mathrm{P,N})} c_{kI}^* c_{kJ} \sum_{m,n=1}^{P_u} h_{mn}^M \, \langle \; | \prod_{p=1}^{N_p \in \mathcal{S}_I} \prod_{\overline{p}=N_p+1}^{N_p \in \mathcal{S}_I + N_{\overline{p}} \in \overline{\mathcal{T}}_I} a_{\overline{p}} a_p \, a_m^\dagger a_n \prod_{q=1}^{N_p \in \mathcal{S}_J} \prod_{\overline{q}=N_p+1}^{N_p \in \mathcal{S}_J + N_{\overline{p}} \in \overline{\mathcal{T}}_J} a_q^\dagger a_{\overline{q}}^\dagger \; | \; \rangle \tag{16}$$

with $N_{p(\overline{p})}$ the number of electrons occupying the string $\mathcal{S}_K(\overline{\mathcal{T}}_K)$ and $N = N_p + N_{\overline{p}}$ in a given string combination (see Eq. (5)) forming a Slater determinant. The interaction constant thus results from the contraction of CI densities, molecular integrals and coupling coefficients.

Implementation

The one-electron operator in Eq. (14) can be written more explicitly for the component along the molecular axis (*i.e.*, $l = z$) using

$$\left(\frac{\boldsymbol{\alpha} \times \mathbf{r}}{r^5} \right)_z r_z = \alpha_1 \frac{r_2 r_3}{r^5} - \alpha_2 \frac{r_1 r_3}{r^5} \tag{17}$$

with r_i the ith cartesian component of the electronic position vector $\mathbf{r}$. The components of the electric-field gradient, a second-rank tensor, are

$$\frac{1}{q} \frac{\partial}{\partial r_i} E_j(\mathbf{r}) = -3 \frac{r_i r_j}{r^5} \tag{18}$$

for a point charge q and $i \neq j$. We calculate atomic integrals over the two terms on the right-hand side of Eq. (17) as integrals over corresponding components of electric field gradients, as

$$\iiint_\mathcal{V} \frac{r_i r_j}{r^5} d^3r = -\frac{1}{3} \iiint_\mathcal{V} \frac{\partial}{\partial r_i} \frac{r_j}{r^3} \, d^3r. \tag{19}$$

The non-vanishing integrals over the full four-spinors are then those of the generic type

$$\left\langle \Psi^L \left| \sigma_k \frac{r_i r_j}{r^5} \right| \Psi^S \right\rangle \tag{20}$$

with σ_k the kth spin-Pauli matrix and the small-component wavefunction Ψ^S in the ket-vector of the same spatial parity as the large-component wavefunction Ψ^L in the bra-vector, since the α matrices couple large and small components of the four-spinors. This can only be the case if Ψ^L and Ψ^S come from different atomic contributions to a molecular spinor, reflecting the fact that the molecular spinors are not parity eigenfunctions.

After the computation of these integrals in the atomic spinor basis, an integral transformation is performed into the molecular spinor basis using the expansion coefficients from a preceding DCHF calculation, yielding one-electron integrals of the type h^M_{pq} in Eq. (16).

Other interaction constants

The electron EDM interaction constant is evaluated in accord with stratagem II of Lindroth et al. [30] as an effective one-electron operator via the squared electronic momentum operator,

$$W_d := \frac{2\imath c}{\Omega\, e\hbar} \left\langle \sum_{j=1}^{n} \gamma_j^0 \gamma_j^5\, \vec{p}_j{}^2 \right\rangle_{\psi_\Omega} \tag{21}$$

with n the number of electrons, as described in greater detail in reference [19]. It is related to the EDM effective electric field as $E_{\text{eff}} = \Omega\, W_d$.

The eN-SPS interaction constant is defined and implemented [31] as

$$W_{\mathcal{P},\mathcal{T}} := \frac{\imath}{\Omega} \frac{G_F}{\sqrt{2}} Z \left\langle \sum_{j=1}^{n} \gamma_j^0 \gamma_j^5\, \rho_N(\vec{r}_j) \right\rangle_{\psi_\Omega} \tag{22}$$

where G_F is the Fermi constant, Z is the proton number and $\rho_N(\vec{r}_j)$ is the nuclear charge density at position $\vec{r}_j$, normalized to unity.

In addition to the above $\mathcal{P},\mathcal{T}$-odd interaction constants we investigate in the present work magnetic hyperfine interaction which serves as an evaluation quantity for the quality of electronic wavefunctions, since spin density close to nuclei is probed. The parallel hyperfine constant is defined as follows:

$$A_{||} = \frac{\mu_A}{I\Omega} \left\langle \sum_{i=1}^{n} \left(\frac{\vec{\alpha_i} \times \vec{r}_{iA}}{r^3_{iA}} \right)_z \right\rangle_{\psi_\Omega} \tag{23}$$

where A designates a nucleus, $\vec{\alpha}$ is a vector of Dirac matrices, and $\vec{r}_{iA}$ is the position vector relative to nucleus A. Further details can be found in reference [16].

APPLICATION TO TAN

Technical details

General

A local version of the `DIRAC11` program package [25] has been used for all presented calculations. This version has been extended to allow for the calculation of expectation values over the various property operators reported in this work (see references [16, 19, 31]), in the present case the nuclear magnetic quadrupole moment interaction. Correlated wavefunctions were obtained with the `KR CI` module [24]. In all calculations the speed of light was set to 137.0359998 a.u.

Atomic basis sets

Fully uncontracted all-electron atomic Gaussian basis sets of triple-ζ quality were used for the description of electronic shells. For tantalum we used Dyall's basis set [32, 33] and for nitrogen

the Dunning cc-pVTZ-DK set [34]. For tantalum valence- and core-correlating exponents were added to the basic triple-ζ set, amounting to $\{30s, 24p, 15d, 11f, 3g, 1h\}$ uncontracted functions. In electron-correlated calculations the virtual spinor space has been consistently truncated at 30 a.u.

Molecular spinors

Kramers-paired four-spinors have been obtained from Dirac-Coulomb Hartree-Fock calculations including 4-index integrals (unapproximated) over Small spinor components. The chosen model used a Fock operator where occupation numbers were averaged by evenly distributing 2 electrons over the valence spinors with the leading character Ta(s_σ) and a pair of Ta(d_δ). Such a basis set of molecular spinors is expected to yield a balanced description of ground Σ and first excited Δ states of the TaN molecule while being very similar to excited-state specific Δ spinors. For comparison, we have also tested the latter by restricting one electron to Ta(s_σ) and one electron to Ta(d_δ) and call them Δ-spinors.

Configuration spaces

We exploit the Generalized Active Space (GAS) concept for defining CI wavefunctions of varying quality. Figure 1 shows the partitioning of the space of Kramers-paired spinors into seven subspaces, six of which are active for replacements of either particle or hole type. Based on this

FIG. 1: Generalized Active Space models for TaN CI wavefunctions. The parameters m, n, p, q are defined in subsection and determine the occupation constraints of the subspaces of Kramers-paired spinors. The molecular spinors are denoted according to their principal atomic character. The space with 110 virtual Kramers pairs is comprised by all canonical DCHF spinors below an energy of 30 E_H.

GAS #		# of Kramers pairs	accumulated # of electrons min.	max.
VI	*Virtual*	110	26	26
V	*Ta: 6p,7s,7p,π Ta: 6s, 5dδ*	K	26−q	26
IV	*N: 2p (Ta: d)*	3	24−p	24
III	*N: 2s (Ta: d)*	1	18−n	18
II	*Ta: 5s, 5p*	4	16−m	16
I	*Ta: 4s, 4p*	4	8−k	8
	Frozen core	(27)		

partitioning and five parameters (k, m, n, p, q) which define the accumulated occupation con-

straints of the subspaces, we choose a number of different CI wavefunction models for our calculations:

parameter values	correlation model acronym	space dimension ($\Omega = 1$)
$k = 0, m = 0, n = 2, p = 2, q = 2$	MR_K-CISD(10)	24,467,439
$k = 0, m = 0, n = 2, p = 2, q = 3$	MR_K-CISDT(10)	156,703,118
$k = 0, m = 0, n = 2, p = 3, q = 2$	MR_K^{+T}-CISD(10)	345,490,884
$k = 0, m = 1, n = 2, p = 2, q = 2$	$MR_K^{'}$-CISD(18)	79,033,385
$k = 0, m = 2, n = 2, p = 2, q = 2$	MR_K-CISD(18)	102,823,317
$k = 0, m = 2, n = 2, p = 2, q = 3$	MR_K-CISDT(18)	691,737,264
$k = 0, m = 1, n = 2, p = 3, q = 2$	$MR_K^{'+T}$-CISD(18)	1,616,196,776
$k = 0, m = 2, n = 2, p = 3, q = 2$	MR_K^{+T}-CISD(18)	2,581,590,063
$k = 1, m = 1, n = 2, p = 2, q = 2$	$MR_K^{'}$-CISD(26)	133,599,331

The parameter K (see Fig. 1) has been introduced to define the active valence spinor spaces, and the dimension of the CI space is given for $K = 12$. $K = 3$ (1,492,556 determinants for $\Omega = 1$ in the model MR_3-CISD(10)) includes only the Ta $(6s, 5d_\delta)$ spinors in the fifth active space and thus comprises a minimal model for a balanced description of the ground $\Omega = 0$ state and the excited $\Omega \in \{1, 2, 3\}$ states which derive from $^3\Delta$ and $^1\Delta$ in the Λ-S coupling picture. The different wavefunction models are in addition defined by the number of correlated electrons in total (in parenthesis) and the included maximum excitation ranks, where "SDT" stands for Single, Double, and Triple excitations, as an example.

Hyperfine interaction

For the determination of the nuclear magnetic hyperfine coupling constant we use the tantalum isotope ^{181}Ta for which the nuclear magnetic moment has been determined to be $\mu = 2.361\mu_N$ [35]. Its nuclear spin quantum number is $I = 7/2$.

Results and discussion

Spectroscopic properties

Table I displays character and some properties of the active set of spinors.

The orbital angular momentum projection quantum number λ has been assigned based on a Mulliken population analysis, and the respective mixings of different λ values in a given Kramers pair are correctly reflected by the $\hat{\ell}_z$ expectation values.

Of particular interest is the character of the $\sigma_{6s_{\mathrm{Ta}}}$ spinor, which displays 79% $6s_{\mathrm{Ta}}$, 8% $6p_{z\mathrm{Ta}}$, and 10% $5d_{x^2,y^2,z^2\mathrm{Ta}}$ leading atomic contributions. Since reference [11] draws a comparison with the YbF molecule for estimating $\mathcal{P},\mathcal{T}$-odd matrix elements, we have performed similar DCHF calculations on YbF. Here, the $\sigma_{6s_{\mathrm{Yb}}}$ spinor has 84% $6s_{\mathrm{Yb}}$, 13% $6p_{z\mathrm{Yb}}$, and a few % $5d_{x^2,y^2,z^2\mathrm{Ta}}$ contribution, confirming the assumption made by Flambaum et al. [11] that the p-wave contribution is significantly smaller in TaN. It is noteworthy that our finding is not in accord with the theoretical results of Bernath et al. [14] on this point, where no p-wave contribution has been found in the case of TaN. However, our present DCHF calculations account for spin-orbit interaction in contrast to the scalar relativistic calculations in reference [14].

Earlier internally contracted scalar-relativistic MRCI calculations [14] on TaN electronic states have shown that the wavefunction of the excited $^3\Delta$ state which is of particular interest in the present study contains non-negligible contributions from two types of Triple excitations which we denote using the Kramers pair numbering indices from Table I:

$$(38,39)^2(40)^1 \longrightarrow (41,42)^1(43,44)^2$$
$$(37)^1(38,39)^1(40)^1 \longrightarrow (41,42)^1(43,44)^1(45)^1$$

TABLE I: Characterization of active-space Kramers pairs in terms of orbital angular momentum projection, spinor energy, and principal atomic shell character; the Kramers pairs numbered 29-35 represent the Ta(4f) shell.

No.	$\lvert m_j \rvert$	$\left\lvert \left\langle \hat{\ell}_z \right\rangle_{\varphi_i} \right\rvert$	ε_{φ_i} $[E_H]$	atomic population, Atom(ℓ_λ)
25	1/2	0.000	−3.184	99% Ta(s)
26	1/2	0.623	−2.016	36% Ta(p_σ), 62% Ta(p_π)
27	1/2	0.374	−1.697	57% Ta(p_σ), 37% Ta(p_π)
28	3/2	1.000	−1.668	99% Ta(p_π)
⋮	⋮	⋮	⋮	⋮
36	1/2	0.003	−0.879	81% N(s), 9% Ta(d_σ)
37	1/2	0.287	−0.362	46% N(p_σ), 17% N(p_π), 14% Ta(d_σ), 10% Ta(d_π)
38	1/2	0.713	−0.353	43% N(p_π), 24% Ta(d_π), 18% N(p_σ)
39	3/2	1.001	−0.353	61% N(p_π), 35% Ta(d_π)
40	1/2	0.002	−0.095	79% Ta(s), 10% Ta(d_σ), 8% Ta(p_σ)
41	3/2	1.996	−0.017	100% Ta(d_δ)
42	5/2	2.000	−0.007	100% Ta(d_δ)
43	1/2	0.990	0.022	88% Ta(p_π)
44	3/2	1.001	0.025	90% Ta(p_π)
45	1/2	0.008	0.041	60% Ta(p_σ), 14% Ta(s), 13% Ta(d_σ)
46	1/2	0.023	0.094	86% Ta(s), 13% Ta(d_σ)
47	1/2	0.636	0.103	51% Ta(p_π), 25% Ta(p_σ), 10% Ta(d_π)
48	3/2	1.001	0.113	77% Ta(p_π)
49	1/2	0.342	0.115	36% Ta(p_σ), 26% Ta(p_π), 16% Ta(d_σ)
50	3/2	1.030	0.240	47% Ta(d_π), 34% Ta(p_π), 13% N(p_π)
51	1/2	1.000	0.240	47% Ta(d_π), 34% Ta(p_π), 16% N(p_π)

Here, the superscript denotes an occupation number. Our CI expansions of the type MR_{12}^{+T}-CISD, therefore, include an important subset of Quintuple excitations with respect to the $^1\Sigma$ ground state of TaN which constitute Double excitations with respect to the above triply-excited configurations. These Double excitations are written using the GAS notation from Fig. 1 as

$$\begin{aligned} \mathrm{V}^2 &\longrightarrow \mathrm{VI}^2 \\ \mathrm{IV}^1\mathrm{V}^1 &\longrightarrow \mathrm{VI}^2 \\ \mathrm{III}^1\mathrm{V}^1 &\longrightarrow \mathrm{VI}^2. \end{aligned}$$

Table II shows vertical excitation energies for five low-lying electronic states.

TABLE II: Calculated vertical excitation energies T_v for $\Omega \in \{0, 1, 2, 3\}$ at $R = 3.1806$ a_0

	Correlation model				
State (Ω)	CAS2	CAS-SD2	MR_3-CISD(10)	MR_{12}-CISD(10)	MR_{12}^{+T}-CISD(10)
2	13409	9164	11321	11749	11693
3	2896	3754	3436	5259	5434
2	1214	1977	1801	3597	3772
1	0	917	682	2502	2673
0	3147	0	0	0	0

CAS2 denotes a 2-electron Full CI calculation in the $\sigma_{6s_{\mathrm{Ta}}}$, $\delta_{5d_{\mathrm{Ta}}}$ subspace, and CAS2-SD2 a 2-electron Full CI calculation including all virtual spinors up to an energy of 30 a.u. It becomes clear

that an active spinor space including only the three above-mentioned spinor pairs is insufficient in describing correctly the relative energies of the low-lying states. We, therefore, base all following studies on models of the type MR_{12}.

In Table III we compare calculated spectroscopic constants from different electronic structure models with experiment.

TABLE III: Calculated spectroscopic constants (R_e the equilibrium internuclear distance, ω_e the harmonic vibrational frequency, B_e the rotational constant, and T_e the equilibrium excitation energy) for $\Omega \in \{0, 1, 2, 3\}$ and comparison with experimental values where available

State	Model	R_e [a.u.]	ω_e [cm^{-1}]	B_e [cm^{-1}]	T_e [cm^{-1}]
	av. DCHF	3.115	1163	0.477	0
$^1\Sigma_0^+$	MR_{12}-CISD(10)	3.160	1161	0.464	0
	MR_{12}^{+T}-CISD(10)	3.205	1122	0.451	0
	MR_{12}-CISD(18)	3.136	1184	0.471	0
	MR_{12}-CISD(18)+T	3.181	1134	0.458	0
	Exp.	3.181[b]	1070[a]		0.0
$^3\Delta_1$	MR_{12}-CISD(10)	3.170	1116	0.461	2526
	MR_{12}^{+T}-CISD(10)	3.222	1088	0.446	2598
	MR_{12}-CISD(18)	3.148	1136	0.468	2879
	MR_{12}-CISD(18)+T	3.196	1095	0.454	2967
	Exp.	3.196[b]			2827.2917[b]
$^3\Delta_2$	MR_{12}-CISD(10)	3.169	1117	0.461	3618
$^3\Delta_3$	MR_{12}-CISD(10)	3.168	1119	0.462	5276
$^1\Delta_2$	MR_{12}-CISD(10)	3.153	1123	0.466	11729

[a]Reference [40]
[b]T_0 from Reference [14]

Potential-energy curves for the four lowest-lying electronic states are displayed in Figure 2.

FIG. 2: Potential energy curves for five lowest-lying electronic states of TaN, using the CI model MR_{12}-CISD(10), cutoff 30 a.u. The energy offset is -15671 E_H.

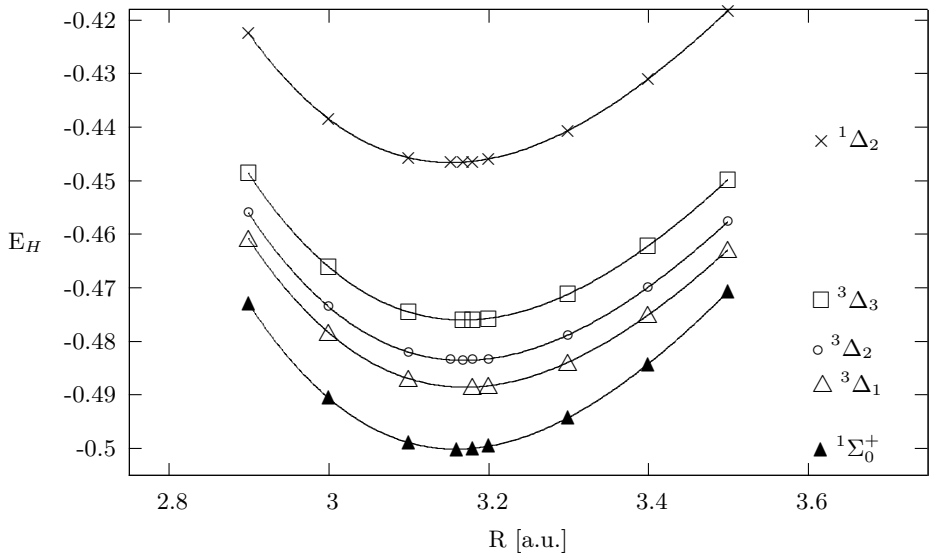

The additional selected Triple excitations stretch the lower-lying potential energy curves significantly, presumably owing to partial depopulation of bonding spinors. This stretching is, not surprisingly, accompanied by a decrease in harmonic vibrational frequency. The opposite is observed when including determinants with one and two holes in the $5s_{\mathrm{Ta}}$ and $5p_{\mathrm{Ta}}$ spinors in the wavefunction expansion. This partial depopulation of compact tantalum outer-core shells results in an increased effective nuclear electric potential "seen" by the bonding valence electrons and is therefore the likely reason for the bond contraction. Both effects are important, and we therefore deduce constants for the lowest two states from the 18-electron model with energies of the individual Born-Oppenheimer points corrected by the energy due to the Triples correction in the 10-electron model. This corrected model is called MR_{12}-CISD(18)+T and yields very accurate equilibrium bond lengths. There remains a deviation from experiment of more than 60 cm^{-1} for the ground-state harmonic vibrational frequency, however.

Since no experimental data are available for the rotation constant, we only mention here that the rotation constant is largely insensitive to different electronic-structure models, the value varying on the order of a few percent.

The equilibrium excitation energy T_e for the first excited ($\Omega = 1$) state is already in quite good agreement with the experimental value for the MR_{12}^{+T}-CISD(10) model. Including outer-core correlations, however, lead to a substantial further improvement, with the MR_{12}-CISD(18)+T model overshooting by only about 170 cm^{-1}.

Since active-space Triple excitations make an important contribution to the static molecular dipole moment of the $\Omega = 1$ state (see Table V), we present in Table IV molecular dipole moments and transition dipole moments computed with the model MR_{12}^{+T}-CISD(10).

TABLE IV: Molecular static electric dipole moments $\left\langle {}^{M}\Lambda_\Omega|\hat{D}_z|{}^{M}\Lambda_\Omega\right\rangle$, transition dipole moments $\left|\left|\left\langle {}^{M}\Lambda'_\Omega|\hat{\vec{D}}|{}^{M}\Lambda_\Omega\right\rangle\right|\right|$, with $\hat{\vec{D}}$ the electric dipole moment operator (both in Debye units), using the model MR_{12}^{+T}-CISD(10). The origin is at the center of mass, and the internuclear distance is $R = 3.1806$ $[a_0]$ (N nucleus placed at $z\vec{e}_z$ with $z > 0$).

${}^{M}\Lambda_\Omega$ State	${}^1\Sigma_0^+$	${}^3\Delta_1$	${}^3\Delta_2$	${}^3\Delta_3$	${}^1\Delta_2$
${}^1\Sigma_0^+$	−3.515				
${}^3\Delta_1$	0.028	−4.809			
${}^3\Delta_2$	0.000	0.085	−4.775		
${}^3\Delta_3$	0.000	0.000	0.087	−4.776	
${}^1\Delta_2$	0.000	0.139	0.114	0.164	−4.000

In the state that will possibly be used for a future EDM measurement, $\Omega = 1$, the molecule has a very large electric dipole moment of about 4.8 Debye. This is for one thing an asset regarding the polarisation of the molecule along an external electric laboratory field. For the other, a large molecular dipole moment also implies a large EDM effective electric field which will be discussed in the following subsection. Transition dipole moments have the expected qualitative agreement with selection rules for electric dipole transitions. The value for $\left|\left|\left\langle {}^3\Delta_1|\hat{\vec{D}}|{}^1\Sigma_0^+\right\rangle\right|\right| \approx 0.03$ Debye is of particular interest. Since $\Delta\Lambda = \pm 2$ for this transition, it should be electric-dipole forbidden. The non-zero value for the transition dipole moment indicates that $\Lambda = 2$ is not an accurate assignment for this excited state and that electronic spin-orbit interaction mixes in states with $\Lambda = 1$, for example a higher-lying ${}^1\Pi_1$ state arising from a $\sigma^1_{6s_{\mathrm{Ta}}}$, $\pi^1_{5d_{\mathrm{Ta}}}$ electronic configuration.

$\mathcal{P},\mathcal{T}$-odd constants and magnetic hyperfine interaction

We proceed with a detailed discussion of the results presented in Table V.

For all three $\mathcal{P},\mathcal{T}$-odd constants the general trend is observable that their value increases with the number of explicitly correlated electrons. Comparing 10-electron with 26-electron models, the increase amounts to roughly 14% for E_{eff}, 12% for $W_{P,T}$, and 14% for W_M, respectively. The effect of Double excitations from the $5s, 5p_{\mathrm{Ta}}$ shells is seen to be negligible for these three

TABLE V: Vertical excitation energy, molecular electric dipole moment, EDM effective electric field, magnetic hyperfine interaction constant, scalar-pseudoscalar electron nucleon interaction constant, and nuclear magnetic quadrupole interaction constant at an internuclear distance of $R = 3.1806$ a$_0$ for $\Omega = 1$

CI Model	T_v [cm^{-1}]	D [Debye]	E_{eff} $[\frac{\text{GV}}{\text{cm}}]$	$A_{\|\|}$ [MHz]	$W_{P,T}$ [kHz]	W_M $[\frac{10^{33}\text{Hz}}{e\,\text{cm}^2}]$
MR$_{12}$-CISD(10)	2502	−5.11	30.1	−3118	27.4	0.633
MR$_{12}$-CISDT(10)	2688	−5.13	29.7	−3092	27.1	0.626
MR$_{12}^{+T}$-CISD(10)	2673	−4.81	31.4	−3067	28.7	0.645
MR$'_{12}$-CISD(18)	1972	−5.18	33.3	−3147	30.3	0.714
MR$_{12}$-CISD(18)	2810	−5.46	33.6	−3059	30.5	0.718
MR$_{12}$-CISDT(18)		−5.49	33.4	−3074	30.3	0.716
MR$_{12}^{'+T}$-CISD(18)		−4.83	35.1	−3025	31.9	0.737
MR$_{12}^{+T}$-CISD(18)		−4.97	35.2	−2917	32.0	0.739
MR$'_{12}$-CISD(26)	1958	−5.18	34.2	−3237	31.1	0.732

properties, indicating that electron correlations of valence and core-valence type are of predominant importance. Since the full 26-electron model is computationally too expensive, the final results will be based on extensive 18-electron results with an additive correction for $4s, 4p_{\text{Ta}}$ core-valence correlation.

Triple excitations into the set of virtual spinors lead to a slight decrease of the $\mathcal{P},\mathcal{T}$-odd constants. However, this correction is a function of the number of correlated electrons and becomes exceedingly small for 18-electron models, not surpassing 1% in any of the $\mathcal{P},\mathcal{T}$-odd properties. Due to the relatively large active spinor space, the model MR$_{12}$-CISDT(18) contains a significant subset of Quadruple and Quintuple excitations with respect to the simple Fermi vacuum for the $\Omega = 0$ electronic ground state. Therefore, the neglected set of Quadruple and Quintuple excitations comes, in a perturbative sense, with large energy denominators. Consequently, such higher excitations (and those beyond) are expected to lead to negligble corrections. We include the calculated external Triples corrections in our final property values.

In subsection we elucidated how a subset of Triple, Quadruple, and Quintuple excitations involving additional holes in the spinors of $2p_{\text{N}}/d_{\text{Ta}}$ character are included in the wavefunction expansion. These atomic contributions to these spinors are strongly mixed by the molecular field, and the additional higher excitations prove to give non-negligible contributions to the $\mathcal{P},\mathcal{T}$-odd properties. These contributions are fairly consistent when comparing 10-electron and 18-electron models. E_{eff} and $W_{P,T}$ are increased by about 5%, the MQM interaction constant by about 3%, respectively. The magnetic hyperfine interaction constant decreases, on the absolute, by about the same percentage.

The magnetic hyperfine coupling constant displays an overall much less systematic behavior than the $\mathcal{P},\mathcal{T}$-odd constants. On the absolute, core-valence correlations from the $5s, 5p_{\text{Ta}}$ shells leads to a slight increase of $A_{||}$ which, however, is overcompensated when including Double excitations from these shells, leading to an overall decrease. Core-valence correlations from the $(4s, 4p)_{\text{Ta}}$ shells again give a slight increase of $A_{||}$. In total, $A_{||}$ varies by only about 4% between the models MR$_{12}$-CISD(10) and MR$'_{12}$-CISD(26). The effect of including Triple excitations into the virtual spinors leads to a change of less than 1%, which again is unsystematic.

The effect of using Δ-spinors as compared to the state-averaged spinors used throughout in the present study has been investigated with the MR$_{12}$-CISD(18) wavefunction expansion. $A_{||}$ is decreased by 2.7% (or 82 MHz) on the absolute and W_M is decreased by 1.9% (or 0.01 $\frac{10^{33}\text{Hz}}{e\,\text{cm}^2}$), respectively. All other properties (D, E_{eff}, $W_{P,T}$) change by much less than 1%. These corrections, too, will be accounted for in the final estimate.

Table VI presents our final property values for TaN, starting out from the results for model MR$_{12}^{+T}$-CISD(18) and including additive corrections accounting for external Triple excitations, $(4s, 4p)_{\text{Ta}}$ core-valence correlation, and the change to Δ-spinors. The most substantial correction is

to E_{eff} and $W_{P,T}$ due to CV-correlation, leading to an increase by 2.5%, respectively. This contribution is also non-negligible for the magnetic hyperfine constant, but it is here largely coun-

TABLE VI: Final property values, calculated from values in Table V including corrections

D [Debye]	E_{eff} $[\frac{\text{GV}}{\text{cm}}]$	$A_{\|\|}$ [MHz]	$W_{P,T}$ [kHz]	W_M $[\frac{10^{33}\text{Hz}}{e\,\text{cm}^2}]$	
−4.97	35.2	−2917	32.0	0.739	base value from MR_{12}^{+T}-CISD(18)
+0.04	−0.2	−15	−0.2	−0.002	external Triples correction
+0.02	+0.1	+68	+0.2	−0.013	correction for Δ spinors
+0.0	+0.9	−90	+0.8	+0.018	$4s, 4p$ core-valence correlation
−4.91	36.0	−2954	32.8	0.742	**Final value**
Skripnikov *et al.*[a] 4.74	34.9	−3132	31	1.08	
Flambaum *et al.*[b]				≈ 1	estimate

[a]Reference [36]
[b]Reference [11]

teracted by the Δ-spinor correction, which is not the case for E_{eff} or $W_{P,T}$. The MQM interaction constant is left largely unchanged by these corrections, in total.

The comparison with literature values (Skripnikov *el al.* [36]) reveals a good agreement for E_{eff} and $W_{P,T}$, the values displaying differences of about 3% and 5%, respectively. A large part of this difference seems to be due to the $(4s, 4p)_{\text{Ta}}$ core-valence correction which has been taken into account in the present study. The difference for $A_{||}$ is roughly 5.5%, whereas a sizeable deviation is observed for the MQM interaction constant, amounting to $\sim 30\%$. Since the agreement between other $\mathcal{P}, \mathcal{T}$-odd constants is good, there is no obvious reason - such as a substantial difference in the employed molecular wavefunctions - for the observed deviation.

CONCLUSION

We summarize and conclude from our most important findings in the present study. TaN provides an effective electric field of about 36 $[\frac{\text{GV}}{\text{cm}}]$, which is roughly as strong as the field obtained recently for ThF^+ [31, 37], significantly stronger than the field in YbF [38], but about half the field obtained for ThO [16, 39]. The two latter molecules have been used to obtain stronger constraints on possible sources of EDMs [6, 7]. The nuclear MQM interaction constant obtained in the present work is about 0.74 $[\frac{10^{33}\text{Hz}}{e\,\text{cm}^2}]$, smaller than the estimate by Flambaum *et al.* [11] but still large enough to hold promise for investigating BSM $\mathcal{P}, \mathcal{T}$-odd hadron physics. To this end, all of the experimental advantages of using molecules in a low-lying $^3\Delta$ state may be exploited. The very large molecule-frame dipole moment of −4.91 [Debye] we obtain allows for efficient polarization of the molecule in a weak external electric field.

TF and MKN thank the *Agence Nationale de la Recherche* (ANR) through grant no. ANR-BS04-13-0010-01, project "EDMeDM", for financial support. We wish to thank David DeMille (Yale) for helpful discussions.

* Electronic address: timo.fleig@irsamc.ups-tlse.fr
† Electronic address: mk.nayak72@gmail.com
‡ Electronic address: mgk@mf1309.spb.edu

[1] J. Engel, M. J. Ramsey-Musolf, and U. van Kolck. Electric dipole moments of nucleons, nuclei, and atoms: The Standard Model and beyond. *Prog. Part. Nuc. Phys.*, 71:21, 2013.
[2] I. B. Khriplovich and S. K. Lamoreaux. *CP Violation Without Strangeness.* Springer; Berlin, Heidelberg, 1997.
[3] M. Pospelov and A. Ritz. Electric dipole moments as probes of new physics. *Ann. Phys.*, 318:119, 2005.
[4] R. F. Streater and A. S. Wightman. *PCT, Spin Statistics, And All That.* W. A. Benjamin Inc., New York, Amsterdam, 1964.
[5] B. L. Roberts and W. J. Marciano, editors. *Lepton Dipole Moments*, volume 20, chapter 14, pages 519 – 581. Advances Series on Directions in High Energy Physics, World Scientific, New Jersey, 2009. E. D. Commins and D. DeMille, The Electric Dipole Moment of the Electron.
[6] The ACME Collaboration, J. Baron, W. C. Campbell, D. DeMille, J. M. Doyle, G. Gabrielse, Y. V. Gurevich, P. W. Hess, N. R. Hutzler, E. Kirilov, I. Kozyryev, B. R. O'Leary, C. D. Panda, M. F. Parsons, E. S. Petrik, B. Spaun, A. C. Vutha, and A. D. West. Order of Magnitude Smaller Limit on the Electric Dipole Moment of the Electron. *Science*, 343:269, 2014.
[7] J. J. Hudson, D. M. Kara, I. J. Smallman, B. E. Sauer, M. R. Tarbutt, and E. A. Hinds. Improved measurement of the shape of the electron. *Nature*, 473:493, 2011.
[8] B. C. Regan, E. D. Commins, C. J. Schmidt, and D. DeMille. New Limit on the Electron Electric Dipole Moment. *Phys. Rev. Lett.*, 88:071805, 2002.
[9] M. D. Swallows, T. H. Loftus, W. C. Griffith, B. R. Heckel, E. N. Fortson, and M. V. Romalis. Techniques used to search for a permanent electric dipole moment of the ^{199}Hg atom and the implications for CP violation. *Phys. Rev. A*, 87:012102, 2013.
[10] O. P. Sushkov, V. V. Flambaum, and I. B. Khriplovich. Possibility of investigating P- and T-odd nuclear forces in atomic and molecular experiments. *Sov. Phys. JETP*, 60:873, 1984.
[11] V. V. Flambaum, D. DeMille, and M. G. Kozlov. Time-Reversal Symmetry Violation in Molecules Induced by Nuclear Magnetic Quadrupole Moments. *Phys. Rev. Lett.*, 113:103003, 2014.
[12] R. J. Crewther, P. di Vecchia, G. Veneziano, and E. Witten. Chiral estimate of the electric dipole moment of the neutron in quantum chromodynamics. *Phys. Lett. B*, 88:123, 1979.
[13] J. F. Gunion and D. Wyler. Inducing a large neutron electric dipole moment via a quark chromoelectric dipole moment. *Phys. Lett. B*, 248:170, 1990.
[14] R. S. Ram, J. Liévin, and P. F. Bernath. Emission Spectroscopy and *ab initio* Calculations for TaN. *J. Mol. Spectrosc.*, 215:275, 2002.
[15] A. C. Vutha, B. Spaun, Y. V. Gurevich, N. R. Hutzler, E. Kirilov, J. M. Doyle, G. Gabrielse, and D. DeMille. Magnetic and electric dipole moments of the $H\,^3\Delta_1$ state in ThO. *Phys. Rev. A*, 84:034502, 2011.
[16] T. Fleig and M. K. Nayak. Electron electric dipole moment and hyperfine interaction constants for ThO. *J. Mol. Spectrosc.*, 300:16, 2014.
[17] L. V. Skripnikov, A. N. Petrov, and A. V. Titov. Communication: Theoretical study of ThO for the electron electric dipole moment search. *J. Chem. Phys.*, 139:221103, 2013.
[18] K. C. Cossel, D. N. Gresh, L. C. Sinclair, T. Coffrey, L. V. Skripnikov, A. N. Petrov, N. S. Mosyagin, A. V. Titov, R. W. Field, E. R. Meyer, E. A. Cornell, and J. Ye. Broadband velocity modulation spectroscopy of HfF^+: Towards a measurement of the electron electric dipole moment. *Chem. Phys. Lett.*, 546:1, 2012.
[19] T. Fleig and M. K. Nayak. Electron electric-dipole-moment interaction constant for HfF^+ from relativistic correlated all-electron theory. *Phys. Rev. A*, 88:032514, 2013.
[20] A. E. Leanhardt, J. L. Bohn, H. Loh, P. Maletinsky, E. R. Meyer, L. C. Sinclair, R. P. Stutz, and E. A. Cornell. High-resolution spectroscopy on trapped molecular ions in rotating electric fields: A new approach for measuring the electron electric dipole moment. *J. Mol. Spectrosc.*, 270:1, 2011.
[21] E. R. Meyer and J. L. Bohn. Prospects for an electron electric-dipole moment search in metastable ThO and ThF^+. *Phys. Rev. A*, 78:010502, 2008.
[22] T. Fleig, J. Olsen, and L. Visscher. The generalized active space concept for the relativistic treatment of electron correlation. II: Large-scale configuration interaction implementation based on relativistic 2- and 4-spinors and its application. *J. Chem. Phys.*, 119:2963, 2003.
[23] T. Fleig, H. J. Aa. Jensen, J. Olsen, and L. Visscher. The generalized active space concept for the relativistic treatment of electron correlation. III: Large-scale configuration interaction and multiconfiguration self-consistent-field four-component methods with application to UO_2. *J. Chem. Phys.*, 124:104106, 2006.
[24] S. Knecht, H. J. Aa. Jensen, and T. Fleig. Large-Scale Parallel Configuration Interaction. II. Two- and four-component double-group general active space implementation with application to BiH. *J.*

Chem. Phys., 132:014108, 2010.

[25] DIRAC, a relativistic ab initio electronic structure program, Release DIRAC11 (2011), written by R. Bast, H. J. Aa. Jensen, T. Saue, and L. Visscher, with contributions from V. Bakken, K. G. Dyall, S. Dubillard, U. Ekström, E. Eliav, T. Enevoldsen, T. Fleig, O. Fossgaard, A. S. P. Gomes, T. Helgaker, J. K. Lærdahl, J. Henriksson, M. Iliaš, Ch. R. Jacob, S. Knecht, C. V. Larsen, H. S. Nataraj, P. Norman, G. Olejniczak, J. Olsen, J. K. Pedersen, M. Pernpointner, K. Ruud, P. Sałek, B. Schimmelpfennig, J. Sikkema, A. J. Thorvaldsen, J. Thyssen, J. van Stralen, S. Villaume, O. Visser, T. Winther, and S. Yamamoto (see http://dirac.chem.vu.nl).

[26] J. Loras, S. Knecht, H. J. Å. Jensen, and T. Fleig. Effect of the spin-other-orbit interaction on excitation energies in correlated atomic and molecular calculations. The atoms Ti, Zr, Hf, and their monohydrides TiH, ZrH, HfH, 2012. Manuscript in preparation.

[27] I. B. Khriplovich. A bound on the proton electric dipole moment derived from atomic experiments. *Sov. Phys. JETP*, 71:51, 1976.

[28] T. Fleig and C. M. Marian. *Ab Initio* Calculation of Ω-Splittings and Rovibronic States of the PtH and PtD Molecules. *J. Mol. Spectrosc.*, 178:1, 1996.

[29] M. G. Kozlov and L. N. Labzowsky. Parity violation effects in diatomics. *J. Phys. B*, 28:1933, 1995.

[30] E. Lindroth, B. W. Lynn, and P. G. H. Sandars. Order α^2 theory of the atomic electric dipole moment due to an electric dipole moment on the electron. *J. Phys. B*, 22:559, 1989.

[31] M. Denis, M. Nørby, H. J. Aa. Jensen, A. S. P. Gomes, M. K. Nayak, S. Knecht, and T. Fleig. Theoretical study on ThF^+, a prospective system in search of time-reversal violation. *New J. Phys.*, 17:043005, 2015.

[32] K. G. Dyall. Relativistic double-zeta, triple-zeta, and quadruple-zeta basis sets for the 5d elements Hf-Hg. *Theoret. Chim. Acta*, 112:403, 2004.

[33] K. G. Dyall and A. S. P. Gomes. Revised relativistic basis sets for the 5d elements Hf-Hg. *Theoret. Chim. Acta*, 125:97, 2010.

[34] T. H. Jr. Dunning. Gaussian basis sets for use in correlated molecular calculations. I. the atoms boron through neon and hydrogen. *J. Chem. Phys.*, 90:1007, 1989.

[35] L. C. Erich, A. C. Gossard, and R. L. Hartless. Magnetic moment of ^{181}Ta. *J. Chem. Phys.*, 59:3911, 1973.

[36] L. V. Skripnikov, A. N. Petrov, N. S. Mosyagin, A. V. Titov, and V. V. Flambaum. TaN molecule as a candidate for the search for a T,P-violating nuclear magnetic quadrupole moment. *Phys. Rev. A*, 92:012521, 2015.

[37] L. V. Skripnikov A. V. Titov. Theoretical study of ThF^+ in the search for T,P-violation effects: Effective state of a Th atom in ThF^+ and ThO compounds. *Phys. Rev. A*, 91:042504, 2015.

[38] N. S. Mosyagin, M. G. Kozlov, and A. V. Titov. *J. Phys. B*, 31:L763, 1998.

[39] L. V. Skripnikov and A. V. Titov. Theoretical study of ThO for the electron electric dipole moment search: Electronic properties of $H^3\Delta_1$ in ThO. *J. Chem. Phys.*, 142:024301, 2015.

[40] M. Zhou and L. Andrews. Reactions of Laser-Ablated Niobium, Tantalum, and Rhenium Atoms with Nitrogen Atoms and Molecules. Infrared Spectra and Density Functional Calculations of the Metal Nitride and Dinitride Molecules. *J. Phys. Chem. A*, 102:9061, 1998.